0013-7227/08/$15.00/0
Printed in U.S.A.

Endocrinology 149(2):558–564

doi: 10.1210/en.2007-0805

Functional Vitamin D Receptor (VDR) in the T-Tubules of Cardiac Myocytes: VDR Knockout Cardiomyocyte Contractility

Daniel X. Tishkoff, Karl A. Nibbelink, Kristina H. Holmberg, Loredana Dandu, and Robert U. Simpson

Department of Pharmacology, University of Michigan Medical School, Ann Arbor, Michigan 48109

We have previously shown that the active form of vitamin D, 1,25 dihydroxyvitamin D3 [1,25$(OH)_2D_3$], has both genomic and rapid nongenomic effects in heart cells; however, the subcellular localization of the vitamin D receptor (VDR) in heart has not been studied. Here we show that in adult rat cardiac myocytes the VDR is primarily localized to the t-tubule. Using immunofluorescence and Western blot analysis, we show that the VDR is closely associated with known t-tubule proteins. Radioligand binding assays using ^{3}H-labeled 1,25$(OH)_2D_3$ demonstrate that a t-tubule membrane fraction isolated from homogenized rat ventricles contains a 1,25$(OH)_2D_3$-binding activity similar to the classic VDR. For the first time, we show that cardiac myocytes isolated from VDR knockout mice show accelerated rates of contraction and relaxation as compared with wild type and that 1,25$(OH)_2D_3$ directly affects contractility in the wild-type but not the knockout cardiac myocyte. Moreover, we observed that acute (5 min) exposure to 1,25$(OH)_2D_3$ altered the rate of relaxation. A receptor localized to t-tubules in the heart is ideally positioned to exert an immediate effect on signal transduction mediators and ion channels. This novel discovery is fundamentally important in understanding 1,25$(OH)_2D_3$ signal transduction in heart cells and provides further evidence that the VDR plays a role in heart structure and function. (*Endocrinology* 149: 558–564, 2008)

THE ACTIVE FORM of vitamin D, 1,25 dihydroxyvitamin D3 [1,25$(OH)_2D_3$; calcitriol], has been shown to have direct effects in many different cell types through its action on the vitamin D receptor (VDR). Although the heart has not been thought of as a traditional target tissue, there is a growing body of evidence that 1,25$(OH)_2D_3$ plays a crucial role in heart structure and function (1–3). In animal models, 1,25$(OH)_2D_3$ deficiency causes significant increases in contraction and relaxation rates of isolated perfused rat hearts and causes hypertension in mice (4, 5). Furthermore, ablation of the VDR in mice and vitamin D deficiency in rats leads to cardiac hypertrophy and fibrosis (2, 5–8). Normalization of calcium levels in VDR null mice with a high-calcium high-phosphate rescue diet does not prevent cardiac hypertrophy (8).

Traditionally the VDR has been characterized as a nuclear steroid receptor that modulates gene transcription on binding of its ligand 1,25$(OH)_2D_3$. In this regard we previously showed that 1,25$(OH)_2D_3$ suppresses expression of atrial natriuretic peptide and c-*myc* and induces expression of myotrophin in cardiac myocytes (6). Besides regulating gene expression via the nuclear VDR, 1,25$(OH)_2D_3$ has been shown to exert fast, nongenomic responses involving stimulation of transmembrane signal transduction pathways through uncharacterized and putative membrane-associated receptors (9–11). Also, there is evidence that the rapid responses to 1,25$(OH)_2D_3$ in cardiac and skeletal muscle cells involve the influx of calcium through voltage gated calcium channels by activation of G protein-coupled second messenger systems (10, 12).

Recently the VDR has been found in isolated membrane fractions of both chick intestinal cells and chick embryonic skeletal muscle cells (12, 13). Here we show that in adult rat and mouse cardiomyocyte VDR is located in the t-tubular structure, and a portion of VDR translocates to the nucleus after treatment of cardiomyocytes with 1,25$(OH)_2D_3$. Moreover, we show that ablation of VDR in mice results in chronic changes in contractile kinetics and that 1,25$(OH)_2D_3$ has rapid effects on myocyte contraction that are absent in VDR-KO myocytes.

First Published Online November 1, 2007

Abbreviations: COX, Cytochrome oxidase; DHPR, dihydropyridine receptor; +dl/dt, relaxation; −dl/dt, contraction; ER, estrogen receptor; 40K, 40,000-g membrane; KO, knockout; KREBS, Krebs-buffered solution; LTCC, L-type calcium channel; M199, media 199 supplemented with penicillin/streptomycin; 1,25$(OH)_2D_3$, 1,25 dihydroxyvitamin D3; PBS-T, PBS-Triton X-100; SERCA, sarcoendoplasmic reticulum Ca^{2+}-ATPase; Sp1, specificity protein-1; TBST, Tris-buffered saline containing Tween 20; T-cap, telethonin; TTP, time to peak contraction; TTR, time to relaxation; TTR25%, TTR 25%; TTR75%, TTR 75% relaxation; VDR, vitamin D receptor; WT, wild type.

***Endocrinology* is published monthly by The Endocrine Society (http://www.endo-society.org), the foremost professional society serving the endocrine community.**

Materials and Methods

All procedures involving animals were executed in accordance with the guidelines of the University Committee on the Use and Care of Animals of the University of Michigan. Three-month-old female Sprague Dawley rats (Charles River Laboratory, Wilmington, MA) and 6-month-old VDR-wild-type (WT) or VDR-knockout (KO) mice from a colony originally generated by Dr. Marie Demay (Harvard Medical School, Boston, MA) were used in this study. Mice and rats were housed in the University of Michigan Laboratory Animal Facility in standard cages with a 12-h light, 12-h dark cycle. Mice were fed a high-calcium high-phosphate rescue diet containing 20% lactose, 2% calcium, and 1.25% phosphorous with 2.2 IU vitamin D_3/g (diet TD.96348; Harlan Teklad, Madison, WI) and water *ad libitum*. Rats were fed standard rat chow.

Isolation of rat ventricular myocytes

Ventricular myocytes were isolated from rat hearts as previously described (3). Female Sprague Dawley rats (250–300 g) were pretreated with 0.01 U/kg heparin ip followed 10 min later by a lethal dose of pentobarbital. The heart was quickly removed and mounted on a Langendorf apparatus and retrogradely perfused with Krebs-buffered solution (KREBS) solution containing (in millimoles): 118 NaCl, 4.8 KCl, 1.2 $MgSO_4$ $7H_2O$, 1.0 CaCl2 $2H_2O$, 25 HEPES, 1.2 KH2PO4, and 11 glucose (pH set to 7.4 using NaOH). When the coronary circulation had cleared of blood, perfusion was continued with Ca^{2+}-free KREBS for 3 min, followed by perfusion for a further 30 min with Ca^{2+}-free solution containing 0.25 mg/ml recombinant collagenase (Liberase Blendzyme 1; Roche, Stockholm, Sweden), 12.5 μM $CaCl_2$, and 2.5% trypsin (Life Technologies, Inc., Grand Island, NY). Calcium concentration was gradually increased to 0.75 mM during the digestion. The ventricles were then excised, minced, and gently shaken at 37 C in the collagenase-containing solution. Ventricular cells were collected from this solution at 5-min intervals and resuspended in KREBS containing 1% BSA and 1.75 mM $CaCl_2$. Cells were then plated onto laminin-coated coverslips in DMEM supplemented with 50 U/ml penicillin, 50 μg/ml streptomycin (Pen/Strep, Life Technologies), and 10% serum. Cells were incubated at 37 C for 2 h in 2% CO_2.

Isolation of mouse ventricular myocytes and contraction studies

Mouse myocytes were isolated in a similar fashion by Langendorf retrograde perfusion and digestion essentially as described (http://www.signaling-gateway.org/data/cgi-bin/ProtocolFile.cgi/afcs_PP00000125.pdf?pid=PP00000125) with the following modifications: crude collagenase (Worthington, Freehold, NJ) at 2.4 mg/ml was used for digestion in a solution containing 30 mM taurine and 10 mM BDM (both Sigma, St. Louis, MO; pH 7.0), and digestion was carried out for 10 min and minced ventricles were mixed by pipetting to complete dissociation in the isolation solution containing 1% BSA and plated as above. After 2 h incubation, the plating media were changed to media 199 supplemented with penicillin/streptomycin (M199), 10 mM HEPES, 0.2 mg/ml BSA, and 10 mM glutathione (M199+). Individual coverslips were transferred to a temperature-controlled stimulation chamber containing platinum electrodes mounted to the sides of each well and a glass bottom mounted on a microscope (Nikon, Tokyo, Japan). Myocytes were electrically stimulated (Myopacer, Ionoptix, Milton, MA; 2.5 msec pulse, 0.5 Hz., 4 V), and the chamber was perfused with M199+. Sarcomere shortening was detected using a video-based detection system (Ionoptix, Milton, MA) on intact myocytes. Recordings were made 5, 10, and 15 min after addition of calcitriol (10^{-9} M; Sigma). Ten twitches per myocyte were collected for each sample (n = 20). The shortening transient was indistinguishable over this same time interval in non-stimulated myocytes. Signal averaged data were analyzed to determine resting sarcomere length, peak shortening normalized for resting sarcomere length (percent peak height), time to peak shortening (TTP), time to 25% (TTR25%), 50%, and 75% relaxation (TTR75%), respectively, and maximum normalized shortening and relaxation velocities (+d*l*/d*t*max, −d*l*/d*t*max, respectively).

Immunocytochemistry

Immunocytochemistry was carried out in a method similar to that previously described (6). Briefly, coverslip-plated cells were washed in PBS (pH 7.2) and then fixed in 10% neutral buffered formalin (Sigma) for 10 min, rinsed in PBS, and blocked in 10% donkey serum in PBS-0.05% Triton X-100 (PBS-T). Cells were incubated with mouse VDR antibody (sc-13133; 1:100; Santa Cruz Biotechnology, Santa Cruz, CA), mouse dihydropyridine receptor antibody (DHPR; MA3–921; 1:500; Affinity BioReagents, Golden, CO), rabbit VDR antibody (sc-1008 or sc-1009; 1:100; Santa Cruz), rabbit sarcoplasmic reticulum calcium ATPase antibody [sarcoendoplasmic reticulum Ca^{2+}-ATPase (SERCA)-2; sc-8094; 1:500; Santa Cruz], or rabbit T-cap antibody (sc-20171; Santa Cruz) diluted in 5% donkey serum/PBS-T for 1 h at room temperature, rinsed in PBS, and then incubated with donkey antimouse Alexa488, donkey antirabbit Alexa488, or donkey antigoat Alexa594 (Invitrogen, Carlsbad, CA) secondary antibody diluted in 5% donkey serum in PBS-T for 30 min. Cells were then washed in PBS, incubated with 0.5 μM 4′,6′-diamino-2-phenylindole for 5 min, briefly rinsed, and mounted in ProLong Gold (Invitrogen). Triton X-100 was not included at any stage for the cells shown in Figs. 1, K and L, and 2, A and B. Slides were analyzed with FV-500 imaging software (Olympus, Tokyo, Japan) on a Olympus iX 81 confocal microscope and finalized using Adobe Photoshop (Adobe Systems Inc., San Jose, CA).

Subcellular fractionation of homogenized rat hearts and Western blot

Whole rat hearts were removed, cannulated, and perfused two times with 10 ml ice-cold Dulbecco's PBS and then once with 3 ml of ice-cold TKED lysis buffer [50 mM Tris-HCl, 150 mM KCl, 1.5 mM EDTA, 10 mM dithiothreitol (pH 7.4)] and a 1:100 dilution of protease inhibitor cocktail (Sigma). Ventricles were minced, washed two times in 10 ml TKED lysis buffer and then homogenized on ice with a Tekmar Tissuemizer in 5 volumes (~5 ml) of TKED lysis buffer. The resulting homogenate (whole homogenate) was transferred to a 15-ml Corex tube and centrifuged in a JA-20 rotor (Beckman, Palo Alto, CA) at 8000 rpm (7700 g) for 15 min at 4 C. The pellet was washed with approximately 15 ml of TKED buffer and then resuspended in 2.5 ml TKED lysis buffer (0–7700 g pellet). The supernatant was transferred to a new 15-ml Corex tube and centrifuged in a Beckman JA-20 rotor at 18,200 rpm (40,000 × *g*) for 25 min at 4 C. The resulting membrane pellet was washed once in TKED lysis buffer and then resuspended in 0.1 ml TKED lysis buffer (7,700–40,000 g pellet). The supernatant was transferred to a Beckman Ti 70.1 ultracentrifuge tube and centrifuged in a Beckman Ti 70.1 rotor at 40,000 rpm (110,000 × *g*) for 1 h at 4 C. The resulting pellet was washed once in a few milliliters of TKED lysis buffer and then resuspended in 0.1 ml TKED lysis buffer (40,000–110,000 g pellet); supernatant (cytosol) was transferred to a 15-ml centrifuge tube. Pellets and cytosol were flash frozen in liquid nitrogen. Samples (100 μg) were suspended in 1× Laemmli buffer, boiled for 5 min, and run on a 10% Criterion SDS-PAGE Tris HCl gel (Bio-Rad Laboratories, Hercules, CA) and transferred to an Immobilon-P polyvinyl difluoride membrane (Millipore, Bedford, MA). Membranes were blocked for 1 h in 5% nonfat dry milk and then incubated with primary antibody diluted as follows: VDR (sc-1008; mouse polyclonal; 1:200), L-type calcium channel (LTCC; sc-16230; goat polyclonal; 1:200), SERCA-2 (sc-8094; rabbit polyclonal; 1:100), specificity protein-1 (Sp1; sc-59, rabbit polyclonal; 1:200), or caveolin-3 (sc-5310, mouse monoclonal; 1:200), all from Santa Cruz, DHPR (MA3-921; mouse monoclonal; 1:500) from Affinity BioReagents, and cytochrome oxidase (COX) IV (ab16056; rabbit polyclonal; 1:1000; Abcam, Cambridge, MA). Primary antibodies were diluted in 5% milk/Tris-buffered saline containing 0.05% Tween 20 (TBST) for 1 h at room temperature. After four 5-min washes with TBST, membranes were incubated with a secondary antibody conjugated with horseradish peroxidase (1:1000; GE Healthcare, Indianapolis, IN; NA934 for rabbit primaries, NA931 for mouse primaries, Santa Cruz sc-2020 for goat primary) in 5% milk/TBST for 1 h at room temperature. After four 5-min washes, blots were incubated with Amersham (Piscataway, NJ) or Pierce (Rockford, IL) ECL substrate and exposed to x-ray film.

Radioligand binding assay

Myocardial membranes were prepared as above (subcellular fractionation). The 7,700- to 40,000-g membrane pellet from one homogenized rat heart was washed once in TKED lysis buffer, resuspended in 7.5 ml TKED lysis buffer, and then homogenized with five strokes of a 15-ml Wheaton Potter-Elvejhem tissue grinder. Saturation binding assays with ^{3}H-1,25$(OH)_2D_3$ (specific activity 176 Ci/mmol; GE Healthcare) and 70-μg membranes were done in triplicate in 250 μl of binding buffer of TKED and 100 mM NaCl (pH 7.4) and a 1:100 dilution of protease inhibitor cocktail (Sigma) in 12 × 75 mm borosilicate glass tubes. Nonspecific binding was determined in the presence of cold 1,25$(OH)_2D_3$ (2 μM). Assays were performed at room temperature for 60 min and were then filtered over glass fiber filters (GF-C; Whatman, Middlesesx, UK) and washed two times with 5 ml ice-cold 25 mM Tris HCl (pH 8) and then washed two more times with 15 ml ice-cold 25 mM Tris HCl (pH 8). Filters were placed in 10 ml UniverSol ES (MP Biomedicals, Solon, OH) overnight and then counted in a Beckman LS 5801 liquid scintillation counter. ^{3}H-1,25$(OH)_2D_3$ was obtained from GE Healthcare and was blown down using a nitrogen evaporator and re-

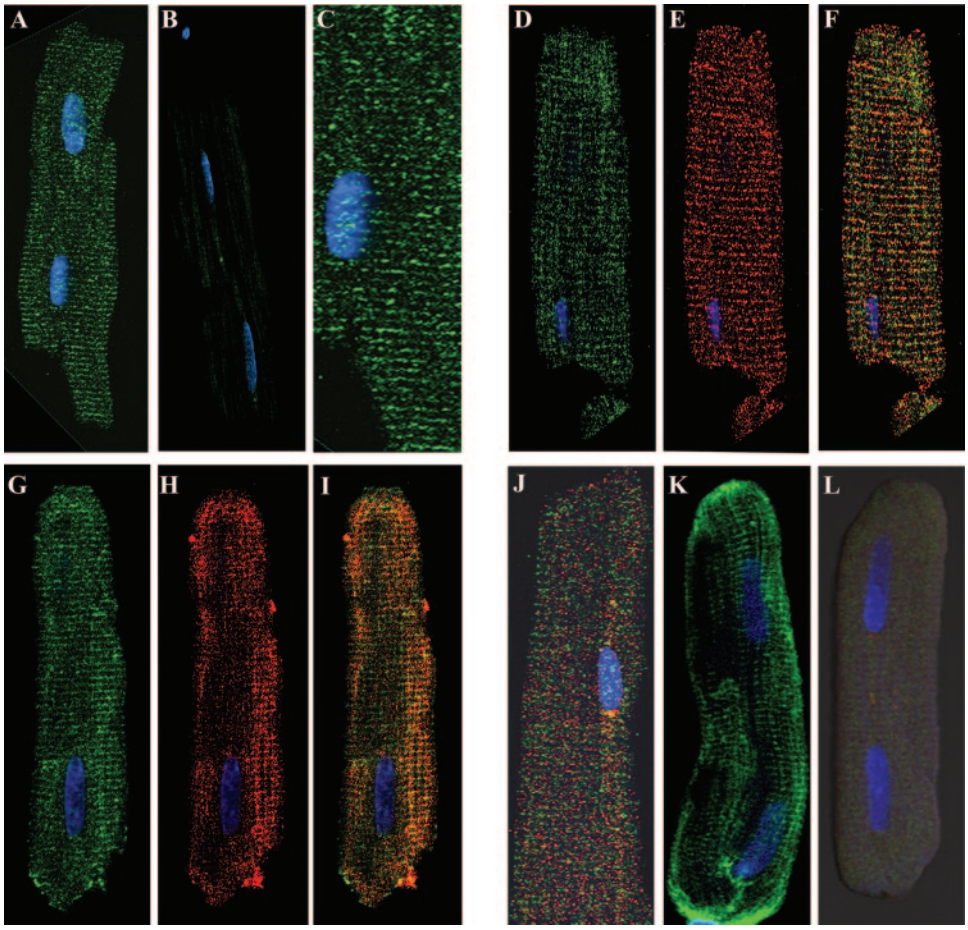

FIG. 1. Immunofluorescent confocal microscopy of adult rat cardiac myocytes. The transverse staining pattern of VDR (sc-13133; mouse monoclonal) is evident at ×40 (A; image enlarged in C). Antimouse secondary antibody alone is shown in B. Double labeling using a different antibody against VDR (sc-1009; rabbit polyclonal, D) and an antibody against DHPR (MA3–921; mouse monoclonal; E) show similar staining patterns, whereas a merge (F) shows colocalization. Double labeling against VDR (sc-1009; rabbit polyclonal; G) and SERCA-2 (sc-8094; goat polyclonal; H) show a similar staining pattern, whereas a merge (I) shows some association. Double labeling using an antibody against T-cap (sc-20171; rabbit polyclonal; *red*) and VDR (sc-1009, rabbit polyclonal, *green*) show dissimilar staining patterns and incomplete overlap in a merged image (J). A third primary VDR antibody, a rabbit polyclonal directed against the C terminus of VDR (sc-1008), is shown in K. A cardiomyocyte incubated with both sc-1008 and a blocking peptide for VDR (sc1008p) is shown in L, demonstrating the specificity of this antibody for VDR.

suspended in ethanol. Cold $1,25(OH)_2D_3$ was obtained from Sigma-Aldrich and was diluted in ethanol.

Statistical analysis

In all experiments significant differences between data sets was determined using two-tailed unpaired Student's *t* test. $P < 0.05$ was considered significant. Data are presented as mean ± SE unless otherwise stated.

Results

Immunocytochemistry and confocal microscopy was used to identify the subcellular location of the VDR in isolated adult heart cells. A strong immunoreactivity was seen in isolated adult rat ventricular cells in the nucleus and also in a repeating pattern of transverse lines throughout the cell (Fig. 1, A, C, D, G, and K). This pattern was consistent between different antibodies directed either at the C terminus (sc-13133) or N terminus (sc-1009) of the VDR. A third antibody (sc 1008) showed similar cell staining, and the specificity of staining was confirmed by using a blocking peptide (Fig. 1, K and L) or omitting the primary antibody (Fig. 1B). This striated pattern is a hallmark of t-tubule components (14, 15), and in fact, VDR appears to closely associate with

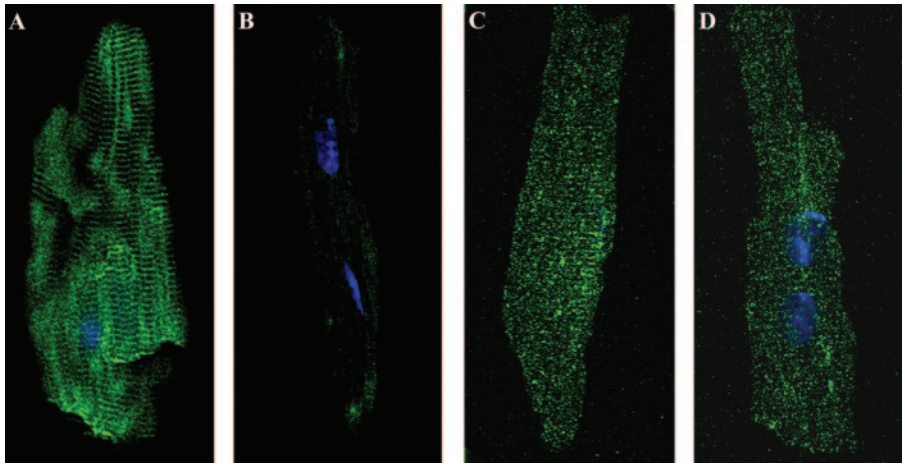

FIG. 2. Immunocytochemistry of WT (A and C) and VDR-KO (B and D) isolated mouse cardiomyocytes after incubation with a mouse monoclonal antibody against VDR (sc-13133; A and B) or a mouse monoclonal antibody against DHPR (E and F). VDR staining is seen in a striated pattern in WT cells (A) and is absent in KO cells (B). DHPR staining corresponding to the localization of t-tubules is seen in both VDR-WT (C) and VDR-KO (D) cells.

known t-tubule proteins. The LTCC, a voltage-sensitive calcium channel, is concentrated along the t-tubule membrane in heart cells and is responsible for the initial calcium current that triggers calcium release from the sarcoplasmic reticulum (16). Double labeling with VDR and DHPR (a component of the LTCC) showed similar patterns of immunoreactivity, suggesting that these two proteins are closely associated (Fig. 1, D, E, and F). SERCA-2, the sarcoplasmic reticulum Ca^{2+}-ATPase, is responsible for removing calcium from cell cytoplasm and causing relaxation in cardiac myocytes, and immunocytochemistry has shown it to be concentrated at the Z-line adjacent to the t-tubule (14). In rat ventricular myocytes SERCA-2 shows a similar pattern of immunoreactivity to that of VDR, and double-labeling experiments suggest a close association of these two proteins (Fig. 1, G, H, and I). To further investigate the localization of these proteins along the Z-line, double-labeling experiments were performed using VDR and the Z-line marker, T-cap [Fig. 1J (17)]. The merged image shows incomplete overlap of these proteins with T-cap, suggesting closer association with the t-tubules than the Z-line.

Immunocytochemistry was also performed on isolated heart cells from VDR-WT and VDR-KO mouse littermates (Fig. 2). Whereas the WT showed the characteristic striated staining pattern (Fig. 2A), no staining was detected in KO cells (Fig. 2B). It is possible that this difference in staining could be a result of gross changes in t-tubule structures and general disorganized expression pattern for t-tubule proteins in VDT-KO cardiomyocytes. DHPR, however, showed the same staining pattern and intensity in both WT (Fig. 2C) and KO cells (Fig. 2D), confirming that the t-tubules structure is not disrupted or absent in KO cells; similar results were found for SERCA-2 (data not shown).

To confirm the presence of VDR within the t-tubules, we fractionated homogenized rat hearts by differential centrifugation using slight modifications of established methods (18–20). Using Western blot analysis, we show that the VDR is enriched in the 7,700- to 40,000-g (40K) membrane fraction and cytosol (Fig. 3A). SERCA-2, LTCC, and DHPR are highly enriched in the 40K fraction, confirming that this fraction contains t-tubules. The fractions were further characterized using the mitochondrial marker COX IV and the nuclear marker Sp1; very little of these markers were found in the 40K fraction (Fig. 3A). Using radioligand binding assays, we show that ^{3}H-1,25$(OH)_2D_3$ binds to the 40K fraction in a specific and saturable manner with a dissociation constant of 0.7×10^{-9} M and a maximal binding capacity of 78.2 fmol/mg (Fig. 3, B and C), consistent with previously published results for both classic and putative membrane VDRs (13, 21). Taken together, the immunocytochemistry along with the Western blot analysis and the binding data provides strong support for a subcellular localization of the VDR within, or adjacent to, the t-tubules.

To examine the function of the VDR in cardiac myocytes, contraction parameters of individual intact cardiomyocytes isolated from VDR-WT and VDR-KO mice were studied by measuring sarcomere shortening (contraction) and relengthening (relaxation) in response to electrical stimulation. Differences between the two cell types were seen in six of the eight parameters measured (Fig. 4). Resting sarcomere length

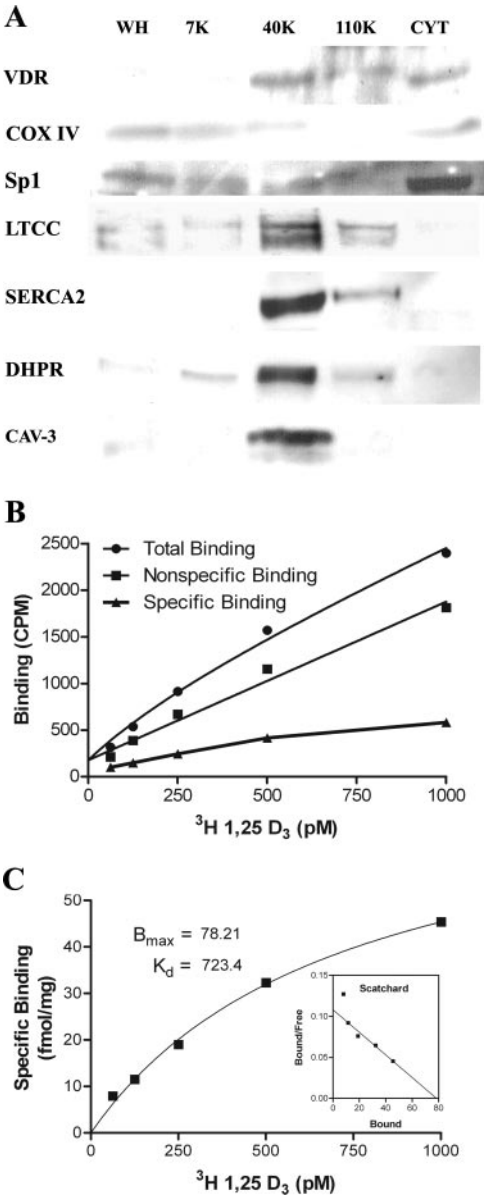

FIG. 3. Western blot of fractionated homogenized rat hearts (A) and ^{3}[H]1,25$(OH)_2D_3$ binding analysis of the t-tubule (40K) fraction (B and C). Fractions analyzed by Western blot (A) include whole homogenate (WH), 0–7,700 g (7K), 7,700–40,000 g (40K), 40,000–110,000 g (110K), and cytosol (CYT). VDR is present in the 40K fraction, which is also enriched for the LTCC, DHPR, SERCA2, and caveolin-3 (CAV-3; A). This fraction shows very little of the mitochondrial marker COX IV or the nuclear marker Sp1 (A). Total, nonspecific, and specific binding of ^{3}[H]1,25$(OH)_2D_3$ to the 40K membrane fraction in counts per minute (CPM) is shown in B. Saturation and Scatchard analysis of ^{3}[H]1,25$(OH)_2D_3$ binding to the 40K fraction shows saturable and specific binding (C). B_{max}, Maximal binding capacity; K_d, dissociation constant.

and peak shortening were unaffected; however, TTP and TTR25%-75% were reduced in VDR-KO cardiomyocytes. Most importantly, the rates of both contraction (−dl/dt) and relaxation (+dl/dt) were significantly increased in the KO cells, compared with the WT cells, indicating hypercontractility in the KO cells. This correlates with our earlier studies in which hypercontractility was observed in isolated per-

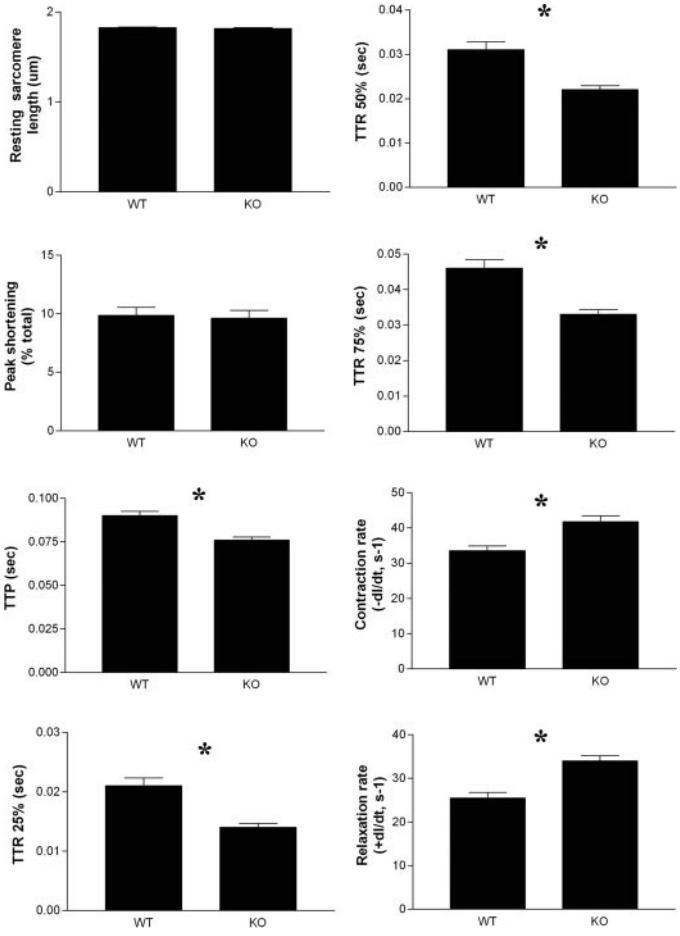

FIG. 4. Baseline contractile differences between ventricular myocytes isolated from 6-month-old VDR-WT and VDR-KO mice (littermates). Ten twitches per myocyte were collected for each sample (n = 20). Resting sarcomere length and peak shortening were unaffected; however, TTP and TTR25%-75% were reduced in VDR-KO cardiomyocytes. Rates of both contraction (−dl/dt) and relaxation (+dl/dt) were significantly increased in the KO (−dl/dt = 41.77 ± 1.649, +dl/dt = 33.97 ± 1.250) cells, compared with the WT (−dl/dt = 25.48 ± 1.258, +dl/dt = 25.48 ± 1.258) cells, indicating hypercontractility in the KO cells. *, $P < 0.05$.

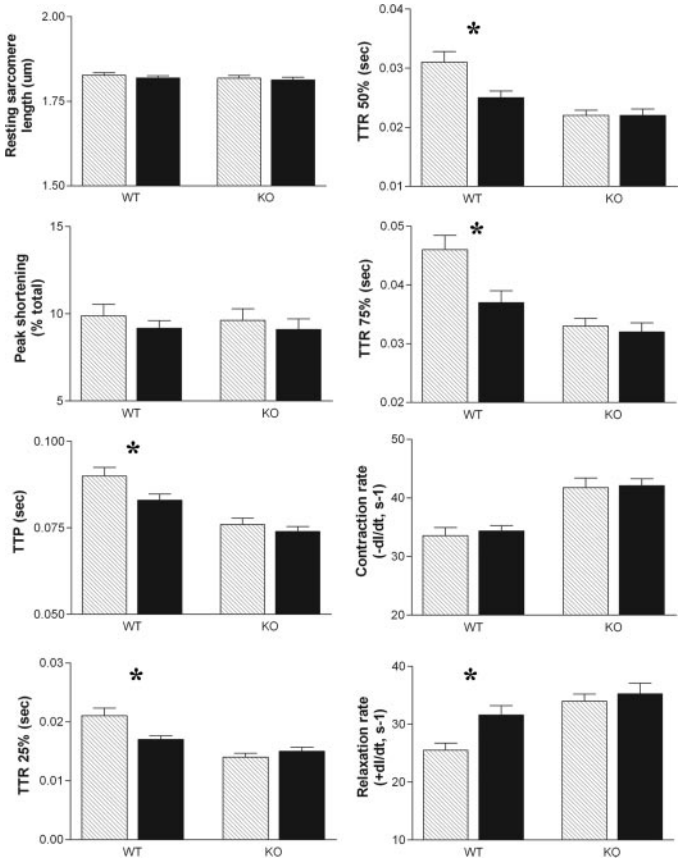

FIG. 5. Effect of $1,25(OH)_2D_3$ on VDR-WT and VDR-KO mouse ventricular myocytes. The VDR-WT and VDR-KO mice are 6-month-old littermates. Ten twitches per myocyte were collected for each sample (n = 20). After treatment with 1 nM $1,25(OH)_2D_3$, WT cells exhibited reduced TTP and TTR75% and unchanged rate of contraction (−dl/dtmax: 33.56 ± 1.375 control, 34.34 ± 0.9398 treated; $P = 0.64$), whereas the rate of relaxation was significantly increased (+dl/dtmax: 25.48 ± 1.258 control, 31.60 ± 1.592 treated; $P < 0.005$). There are no effects after $1,25(OH)_2D_3$ treatment in VDR-KO cells. *Crosshatch bars*, baseline; *black bars*, treated. *, $P < 0.05$.

fused hearts from $1,25(OH)_2D_3$-deficient rats, compared with $1,25(OH)_2D_3$ replete littermates (4, 22). It has previously been shown that VDR-KO mice fed the high-calcium, high-phosphate rescue diet used here maintain normal calcium levels, indicating that these are not secondary effects due to differences in calcium levels in VDR-KO mice (23).

It is now accepted that many steroid hormones induce responses that do not involve gene transcription (24). Nongenomic actions of the VDR have been studied in several cells in which the effects relate to rapid calcium transport (25–27). In isolated rat cardiomyocytes, we previously found that $1,25(OH)_2D_3$ rapidly decreased peak shortening and increased the rate of contraction and relaxation and that this was mediated by increasing the flux of intracellular calcium (3). In this study we found that brief (5 min) exposure to physiological concentrations of $1,25(OH)_2D_3$ had a direct effect on contractility in WT cells that was absent in KO cells (Fig. 5). After treatment with 1 nM $1,25(OH)_2D_3$, WT cells exhibited reduced TTP and TTR75% and unchanged rate of contraction, whereas the rate of relaxation was significantly increased. The lack of any effect after $1,25(OH)_2D_3$ treatment in VDR-KO cells confirms that this process is mediated via the VDR. It is interesting that lack of VDR in KO cells, or deficiency of vitamin D in rats, leads to accelerated rates of contraction and relaxation, whereas treatment with $1,25(OH)_2D_3$ of the WT cells also accelerates the rate of relaxation. These apparently inconsistent results may be due to chronic cellular changes in the $1,25(OH)_2D_3$-deficient rat and the VDR-KO mouse induced over time by inadequate $1,25(OH)_2D_3$ signaling activity.

Figure 6 shows the intensity and localization of VDR in adult rat cardiomyocytes at times zero and after 30 and 60 min treatment with 1 nM $1,25(OH)_2D_3$. The data reveal an increase in overall intensity of VDR fluorescence, suggesting an increased total level of VDR at 30 and 60 min. Figure 6 also shows a consistent increase in the nuclear localization of VDR after treatment with $1,25(OH)_2D_3$ for 30 and 60 min. Immunofluorescence intensity was measured using Fluoview500 (Olympus, Tokyo, Japan) software and plotted as histograms

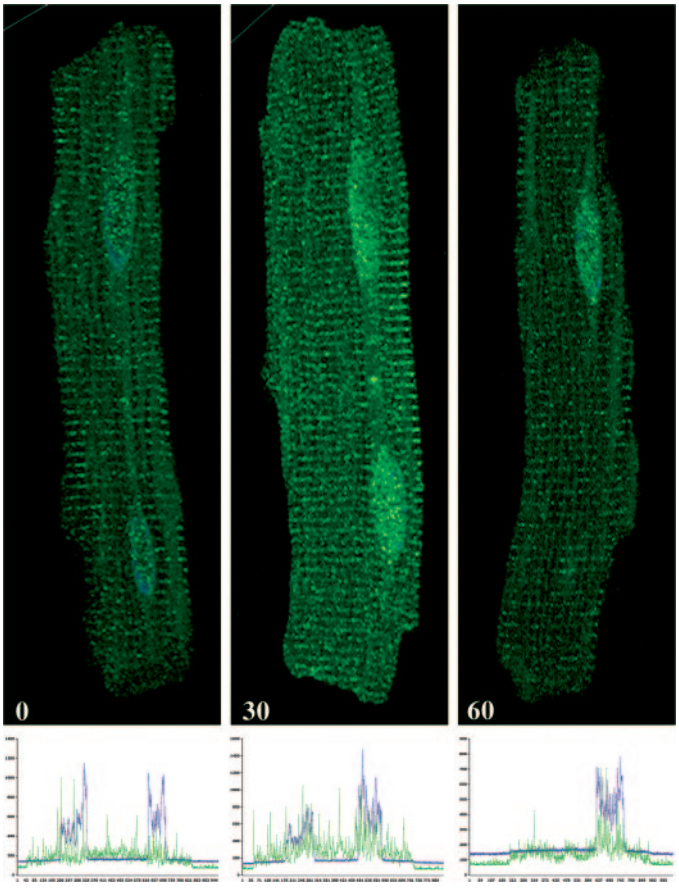

FIG. 6. Effect of $1,25(OH)_2D_3$ (1 nM) on VDR density and location in adult rat cardiomyocytes. Cells were antibody (sc-1009) labeled for VDR by immunofluorescence at time 0, 30, and 60 min after treatment with 1 nM $1,25(OH)_2D_3$. Histograms showing VDR (fluorescein isothiocyanate; *green*) distribution and intensity relative to nuclear staining (4′,6′-diamino-2-phenylindole; *blue*) are shown below each immunofluorescence image.

beneath each immunofluorescence image. The results confirm the increased nuclear localization of VDR after $1,25(OH)_2D_3$ treatment and suggest that both nuclear and membrane actions for $1,25(OH)_2D_3$ could occur and be mediated by the VDR.

Discussion

Rapid nongenomic actions of steroid hormones have been described, and receptors for these rapid actions are broadly believed to be membrane associated, although their characterization remains incomplete (24). The best characterized classic steroid hormone receptor in this respect is the estrogen receptor (ER). In addition to being localized to the cytoplasm, a subpopulation of ERs has been shown to localize to caveolae, cell membrane microdomains important for many signaling pathways (28). The ER is thought to be anchored to the membrane via its association with striatin, a scaffolding protein that contains a caveolin binding domain and is thought to recruit other signaling molecules (29). Recently the VDR has been shown to associate with caveolae-1 microdomains in chick intestinal cells, suggesting a possible mechanism of membrane localization (13). Here we show the t-tubule fraction of rat hearts to be enriched in VDR and caveolin 3 (Fig. 3A), the predominant caveolin subtype in cardiac myocytes (30), suggesting that a similar association may exist in heart cells as well.

In this study we measured contraction parameters of individual intact cardiomyocytes isolated from VDR-WT and VDR-KO mice (Fig. 4). The results show significantly increased rates of contraction and relaxation in KO cells, which might be manifested in live intact animals as changes in heart rate, cardiac output, or other parameters associated with the compensatory phase of the failing heart. We are in the process of testing this hypothesis using echocardiograms of live intact VDR-WT and VDR-KO mice; the results will be presented in a separate publication. The effects seen in VDR-KO animals are unlikely to be secondary to changes in blood pressure because we investigated this possibility in a previous publication, in which we have shown no differences in systolic or mean blood pressure between 3- and 6-month-old VDR-WT and VDR-KO mice (8).

We have also shown a rapid direct effect of treating isolated VDR-WT mouse cardiomyocytes with $1,25(OH)_2D_3$ on contraction rate that was ablated in VDR-KO cells (Fig. 5). This action of $1,25(OH)_2D_3$ was to slow the rate of contraction and increase the rate of relaxation. Whereas the physiological significance of this effect is not clear, this observation demonstrates a rapid direct action of $1,25(OH)_2D_3$ on cardiomyocytes that is dependent on the presence of the VDR.

That a membrane-associated VDR is found within or neighboring the t-tubule structure is important and relevant, given the effects of $1,25(OH)_2D_3$ on heart and the contracting myocyte. It is predominantly the rate of calcium influx through calcium channels that is responsible for the rate and force of myocardial contraction, and these channels are located primarily at the t-tubules in cardiac myocytes (14). There are several mechanisms by which a membrane VDR may affect Ca^{2+} currents in the cell. Previous work from our laboratory provides direct evidence that this process in heart is dependent on the activation of the protein kinase C signaling pathway (3). Other research suggests that the nongenomic action of VDR in the heart involves cAMP (31), protein kinase A (32), β-adrenergic signaling (33), and adenylate cyclase/G proteins (34). Recently we showed that blockade of β-adrenergic signaling or the protein kinase A pathway did not interrupt the acute effect of $1,25(OH)_2D_3$ on rat cardiac myocyte contraction (3). We also showed that $1,25(OH)_2D_3$ induced increased phosphorylation of protein kinase C targets phospholamban B and cardiac troponin I, both of which, through modulation of intracellular Ca^{2+}, would be expected to accelerate relaxation (3).

Earlier studies in our laboratory have shown that lack of vitamin D leads to collagen deposition and cardiac hypertrophy (2, 8). The results presented here support rapid, nongenomic effects of VDR in the heart and localize a major population of the VDR to t-tubules, an ideal position to regulate calcium flux within the cell and modulate contractility.

The acute effect of $1,25(OH)_2D_3$ on cardiac myocytes is primarily to accelerate relaxation [Fig. 5 (Ref. 3)], which suggests that this steroid hormone is important for maintenance of diastolic function. Impaired relaxation of the cardiac myo-

cytes, and subsequent impaired filling of the ventricles, is a main pathological finding in diastolic heart failure. With mounting clinical evidence of a connection between vitamin D and heart failure (27, 35), understanding the role of the VDR in heart is crucial.

Acknowledgments

We thank Drs. Margaret Westfall, William Pratt, and Robert Smith and Mr. William Wilson and Mr. Dustin Robinson, who were instrumental for their inspiration and the success of this work.

Received June 15, 2007. Accepted October 24, 2007.

Address all correspondence and requests for reprints to: Robert U. Simpson, Ph.D., Department of Pharmacology, 1301 MSRB III, 1150 West Medical Center Drive, University of Michigan Medical School, Ann Arbor, Michigan 48109. E-mail: robsim@umich.edu.

This work was supported by National Institutes of Health Grant 5 RO1 HL074894-02 and the Cancer, Diabetes, and Organogenisis Centers at the University of Michigan.

Disclosure Statement: The authors of this manuscript have nothing to declare.

References

1. **Simpson RU, Thomas GA, Arnold AJ** 1985 Identification of 1,25-dihydroxyvitamin D3 receptors and activities in muscle. J Biol Chem 260:8882–8891
2. **Weishaar RE, Kim SN, Saunders DE, Simpson RU** 1990 Involvement of vitamin D3 with cardiovascular function. III. Effects on physical and morphological properties. Am J Physiol 258:E134–E142
3. **Green JJ, Robinson DA, Wilson GE, Simpson RU, Westfall MV** 2006 Calcitriol modulation of cardiac contractile performance via protein kinase C. J Mol Cell Cardiol 41:350–359
4. **Weishaar RE, Simpson RU** 1987 Vitamin D3 and cardiovascular function in rats. J Clin Invest 79:1706–1712
5. **Xiang W, Kong J, Chen S, Cao LP, Qiao G, Zheng W, Liu W, Li X, Gardner DG, Li YC** 2005 Cardiac hypertrophy in vitamin D receptor knockout mice: role of the systemic and cardiac renin-angiotensin systems. Am J Physiol Endocrinol Metab 288:E125–E132
6. **Nibbelink KA, Tishkoff DX, Hershey SD, Rahman A, Simpson RU** 2007 1,25(OH)2-vitamin D3 actions on cell proliferation, size, gene expression, and receptor localization, in the HL-1 cardiac myocyte. J Steroid Biochem Mol Biol 103:533–537
7. **Rahman A, Hershey S, Ahmed S, Nibbelink K, Simpson RU** 2007 Heart extracellular matrix gene expression profile in the vitamin D receptor knockout mice. J Steroid Biochem Mol Biol 103:416–419
8. **Simpson RU, Hershey SH, Nibbelink KA** 2007 Characterization of heart size and blood pressure in the vitamin D receptor knockout mouse. J Steroid Biochem Mol Biol 103:521–524
9. **De Boland AR, Boland RL** 1994 Non-genomic signal transduction pathway of vitamin D in muscle. Cell Signal 6:717–724
10. **Morelli S, Buitrago C, Boland R, de Boland AR** 2001 The stimulation of MAP kinase by 1,25(OH)(2)-vitamin D(3) in skeletal muscle cells is mediated by protein kinase C and calcium. Mol Cell Endocrinol 173:41–52
11. **Norman AW** 2006 Minireview: vitamin D receptor: new assignments for an already busy receptor. Endocrinology 147:5542–5548
12. **Capiati D, Benassati S, Boland RL** 2002 1,25(OH)2-vitamin D3 induces translocation of the vitamin D receptor (VDR) to the plasma membrane in skeletal muscle cells. J Cell Biochem 86:128–135
13. **Huhtakangas JA, Olivera CJ, Bishop JE, Zanello LP, Norman AW** 2004 The vitamin D receptor is present in caveolae-enriched plasma membranes and binds 1α,25(OH)2-vitamin D3 *in vivo* and *in vitro*. Mol Endocrinol 18:2660–2671
14. **Brette F, Orchard C** 2003 T-tubule function in mammalian cardiac myocytes. Circ Res 92:1182–1192
15. **Leach RN, Desai JC, Orchard CH** 2005 Effect of cytoskeleton disruptors on L-type Ca channel distribution in rat ventricular myocytes. Cell Calcium 38: 515–526
16. **Cannell MB, Crossman DJ, Soeller C** 2006 Effect of changes in action potential spike configuration, junctional sarcoplasmic reticulum micro-architecture and altered t-tubule structure in human heart failure. J Muscle Res Cell Motil 27:297–306
17. **Furukawa T, Ono Y, Tsuchiya H, Katayama Y, Bang ML, Labeit D, Labeit S, Inagaki N, Gregorio CC** 2001 Specific interaction of the potassium channel β-subunit minK with the sarcomeric protein T-cap suggests a T-tubule-myofibril linking system. J Mol Biol 313:775–784
18. **Yamaguchi M, Nakajima R** 2002 Role of regucalcin as an activator of sarcoplasmic reticulum Ca2+-ATPase activity in rat heart muscle. J Cell Biochem 86:184–193
19. **Temsah RM, Dyck C, Netticadan T, Chapman D, Elimban V, Dhalla NS** 2000 Effect of β-adrenoceptor blockers on sarcoplasmic reticular function and gene expression in the ischemic-reperfused heart. J Pharmacol Exp Ther 293:15–23
20. **Zucchi R, Ronca-Testoni S, Yu G, Galbani P, Ronca G, Mariani M** 1994 Effect of ischemia and reperfusion on cardiac ryanodine receptors—sarcoplasmic reticulum Ca2+ channels. Circ Res 74:271–280
21. **Nemere I, Dormanen MC, Hammond MW, Okamura WH, Norman AW** 1994 Identification of a specific binding protein for 1α,25-dihydroxyvitamin D3 in basal-lateral membranes of chick intestinal epithelium and relationship to transcaltachia. J Biol Chem 269:23750–23756
22. **Weishaar RE, Simpson RU** 1987 Involvement of vitamin D3 with cardiovascular function. II. Direct and indirect effects. Am J Physiol 253:E675–E683
23. **Li YC, Amling M, Pirro AE, Priemel M, Meuse J, Baron R, Delling G, Demay MB** 1998 Normalization of mineral ion homeostasis by dietary means prevents hyperparathyroidism, rickets, and osteomalacia, but not alopecia in vitamin D receptor-ablated mice. Endocrinology 139:4391–4396
24. **Marcinkowska E, Wiedlocha A** 2002 Steroid signal transduction activated at the cell membrane: from plants to animals. Acta Biochim Pol 49:735–745
25. **Norman AW, Mizwicki MT, Norman DP** 2004 Steroid-hormone rapid actions, membrane receptors and a conformational ensemble model. Nat Rev Drug Discov 3:27–41
26. **Selles J, Boland R** 1991 Rapid stimulation of calcium uptake and protein phosphorylation in isolated cardiac muscle by 1,25-dihydroxyvitamin D3. Mol Cell Endocrinol 77:67–73
27. **Luong KV, Nguyen LT** 2006 Vitamin D and cardiovascular disease. Curr Med Chem 13:2443–2447
28. **Moriarty K, Kim KH, Bender JR** 2006 Minireview: estrogen receptor-mediated rapid signaling. Endocrinology 147:5557–5563
29. **Lu Q, Pallas DC, Surks HK, Baur WE, Mendelsohn ME, Karas RH** 2004 Striatin assembles a membrane signaling complex necessary for rapid, nongenomic activation of endothelial NO synthase by estrogen receptor α. Proc Natl Acad Sci USA 101:17126–17131
30. **Tang Z, Scherer PE, Okamoto T, Song K, Chu C, Kohtz DS, Nishimoto I, Lodish HF, Lisanti MP** 1996 Molecular cloning of caveolin-3, a novel member of the caveolin gene family expressed predominantly in muscle. J Biol Chem 271:2255–2261
31. **Selles J, Boland R** 1991 Evidence on the participation of the 3′,5′-cyclic AMP pathway in the non-genomic action of 1,25-dihydroxy-vitamin D3 in cardiac muscle. Mol Cell Endocrinol 82:229–235
32. **Santillan GE, Boland RL** 1998 Studies suggesting the participation of protein kinase A in 1, 25(OH)2-vitamin D3-dependent protein phosphorylation in cardiac muscle. J Mol Cell Cardiol 30:225–233
33. **Santillan GE, Vazquez G, Boland RL** 1999 Activation of a β-adrenergic-sensitive signal transduction pathway by the secosteroid hormone 1,25-(OH)2-vitamin D3 in chick heart. J Mol Cell Cardiol 31:1095–1104
34. **Selles J, Bellido T, Boland R** 1994 Modulation of calcium uptake in cultured cardiac muscle cells by 1,25-dihydroxyvitamin D3. J Mol Cell Cardiol 26:1593–1599
35. **Zittermann A, Schleithoff SS, Koerfer R** 2006 Vitamin D insufficiency in congestive heart failure: why and what to do about it? Heart Fail Rev 11:25–33

Endocrinology **is published monthly by The Endocrine Society (http://www.endo-society.org), the foremost professional society serving the endocrine community.**